Bo Yu (ed.) (2012). *2012 IEEE Nuclear Science Symposium and Medical Imaging Conference (NSS/MIC): Anaheim, California, USA. October 29 - November 3, 2012* . IEEE, 3344-3346.
DOI: http://dx.doi.org/10.1109/NSSMIC.2012.6551761

Investigation of different Compressed Sensing Approaches for Respiratory Gating in Small Animal CT

Juan Abascal, Alejandro Sisniega, Cristina Chavarrías, Juan José Vaquero, Manuel Desco, and Mónica Abella

***Abstract*– Respiratory gating is necessary in cardio-thoracic small-animal imaging because of the physiological motions that are present during scanning. When applying a low-dose protocol, fewer than 180 noisy projections may be left for the reconstruction of each respiratory phase, leading to streak artifacts. The Prior Image Constrained Compressed Sensing (PICCS) algorithm enables accurate reconstruction of highly undersampled data when a prior image is available. We evaluate three CS algorithms based on the Split-Bregman approach, with different transformations of the prior penalty function: Gradient (TV-PICCS), L1-norm (L1-PICCS), and Wavelet Transform (WT-PICCS), on low-dose data acquired on a micro-CT scanner. All CS methods performed very similarly in terms of noise and resolution, greatly improving filtered back-projection (79 % noise reduction) and eliminating streaks. Wavelet domain was found to be sparser and to show a more natural texture than the commonly used gradient domain.**

I. Introduction

RESPIRATORY gating is necessary in cardio-thoracic small-animal imaging because of the physiological motions that are present during scanning. In order to obtain good quality for every respiratory phase, it is necessary to acquire more data than in the case of standard protocol for static image, which significantly increases the dose. When applying a low-dose protocol, fewer than 180 noisy projections may be left for the reconstruction of each respiratory phase, leading to streak artifacts in the reconstructed images (Fig. 1). In [1, 2] this problem is solved in the analytical framework, using a variation of the McKinnon-Bates method. The algorithm is based on correcting an initial estimate made from the whole data set with the undersampled data for each respiratory phase. The authors show a noise and artifact reduction but it is challenging for the algorithm to correct for the artifacts that are present in the initial estimate [2].

This work was supported in part by projects TEC2008-06715 and TEC2007-64731 (Ministerio de Ciencia e Innovación), EU-FP7 FMTXCT-201792, ARTEMIS S2009/DPI-1802 (Comunidad de Madrid), and European Regional Development Funds (FEDER) and CDTI under the CENIT program (AMIT project, CEN- 20101014).

Juan Abascal, Alejandro Sisniega, Juan José Vaquero, Manuel Desco, and Mónica Abella are with the Departamento de Bioingeniería e Ingeniería Aeroespacial, Universidad Carlos III, Madrid, Spain (e-mail: monica.abella@uc3m.es).

Cristina Chavarrías, Manuel Desco and Juan José Vaquero are with the Instituto de Investigación Sanitaria Gregorio Marañón (IiSGM), Madrid, Spain.

Manuel Desco is with the Centro de Investigación en Red de Salud Mental (CIBERSAM, CIBER CB07/09/0031), 28007 Madrid, Spain.

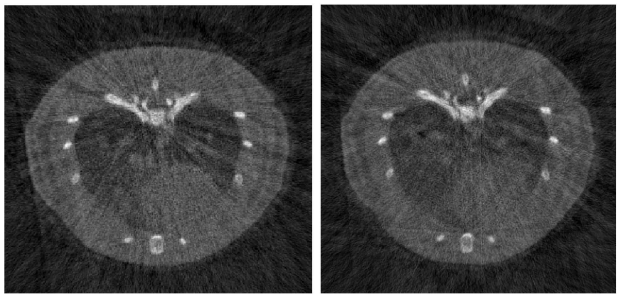

Fig. 1. Central slice of low-dose FDK reconstruction of phases 1 and 3.

In the compressed sensing framework, an image can be accurately reconstructed from few projections using convex optimization if the image is sparse on a transform domain [3, 4]. The most common sparsity domain is the total variation (TV) which efficiently removes noise and artifacts from the image caused by the undersampling. From the large variety of methods available for the solution of L1-penalty functions, the Split-Bregman algorithm has been shown to be optimal [5].

Compared with standard statistical reconstruction methods, TV-based approaches show that around 100 projections are enough to avoid streak artifacts, but the minimization of TV leads to patchy images for high undersampling factors [6].

The Prior Image Constrained Compressed Sensing (PICCS) algorithm is a combination of both strategies, i.e. prior image and sparsity condition, that solves this problem avoiding the patchy texture [7]. The prior in dynamic data is commonly chosen as the image reconstructed from averaging all frames.

The gradient domain is the preferred choice for enforcing the sparsity of the variation of each phase with respect to the prior. However, depending on the application, other transformations such as the pixel domain or the wavelet transformed may be sparser.

In this work we present an evaluation of three CS algorithms based on the Split-Bregman approach, with different transformations of the prior penalty function: Gradient (TV-PICCS), L1-norm (L1-PICCS), and Wavelet Transform (WT-PICCS), on low-dose data acquired on a micro-CT scanner and compared them to an image reconstructed using a filtered back-projection based algorithm (FDK).

II. Methods

A. Data acquisition and low-dose simulation

The algorithms were tested on rodent data acquired with the CT subsystem of an ARGUS/CT (SEDECAL) [8], a cone-beam micro-CT scanner based on a flat panel detector. We obtained 360 views covering 360º, with 32 images of 512×512 pixels (0.2×0.2 mm pixel size) per projection angle and a source voltage of 45 kVp. These high-dose projection data were arranged into four gates using a software-based retrospective gating [9].

To simulate the low-dose case, we randomly took 120 projections from each gate and added Poisson noise by modeling the measurements as independently distributed Poisson random variables:

$$Y_i \sim Poisson\left\{\overline{Y}_i\right\} \quad i=1,\ldots,N \text{ with } \overline{Y}_i = I_i\, e^{-\int_{i,i} u(x,y,z)}, \quad (1)$$

where $u(x,y,z)$ is the unknown energy-dependent attenuation map of the object, and I_i is the intensity emitted by the X-ray source (we used $I_i = 4.5\times10^{-4}$).

A prior image was obtained by adding the four low-dose gates and applying a Gaussian filter with σ=5.

B. Image reconstruction

Let F be the forward operator, u the unknown image, u_p the prior image, f the data, and T_1 and T_2 the transformed sparse domains. The PICCS algorithm is given by

$$\min_u (1-\alpha)\left\|T_1 u\right\|_1 + \alpha\left\|T_2(u-u_p)\right\|_1 \text{ such that } Fu = f, \quad (2)$$

where T_1 is selected as the gradient operator (TV). This selection for T_1 filters out noise while keeping edges.

The prior penalty term helps avoiding the cartoon-like texture and TV is also a common choice for T_2. However, other selections of T_2 might be sparser for this application. We tried the pixel domain (L1-norm), i.e. $T_2 = I$, and the wavelet domain (WT).

In addition, we impose a support constraint that restricts the reconstruction to a circle Ω and a positive constraint [10]. Thus, the reconstruction problem becomes

$$\min_u (1-\alpha)\left\|T_1 u\right\|_1 + \alpha\left\|T_2(u-u_p)\right\|_1 \text{ st } Fu = f, \text{ and } u \ge 0, u \in \Omega. \quad (3)$$

This problem can be efficiently solved using the Split-Bregman formulation by including new variables, d_x, d_y, w, and v that allow for the splitting

$$\begin{aligned}&\min_{d_x,d_y,v,w,u} (1-\alpha)\left\|(d_x,d_y)\right\|_1 + \alpha\left\|w\right\|_1 \\ &+\frac{\mu}{2}\left\|Fu-f^k\right\|_2^2 + \frac{\lambda}{2}\left\|d_x - D_x u - b_x^k\right\|_2^2 + \frac{\lambda}{2}\left\|d_y - D_y u - b_y^k\right\|_2^2 \quad (4)\\ &+\frac{\lambda}{2}\left\|w - T_2(u-u_p) - b_w^k\right\|_2^2 + \frac{\gamma}{2}\left\|v-u-b_v^k\right\|_2^2,\end{aligned}$$

where the variables b_i represent the Bregman iterations that impose the constraints. Note that u is independent of the rest of variables, so the previous equation can be split. Solution of u only involves 2-norm functionals and can be solved exactly and efficiently using a Gaussian-Krylov solver. Solution of d_x, d_y, and w are solved using shrinkage formulas and v by hard thresholding [5].

Low-dose data were reconstructed by using Mangoose [11], an approximation of the FDK method, and three algorithms based on the Split-Bregman approach: TV-PICCS, L1-PICCS, WT-PICCS. Parameters in each algorithm were selected to give comparable resolution properties. We used μ=20, λ=1, γ=0.1 and α =0.8. Our reference standard for evaluation was the result of reconstructing the high-dose data using Mangoose.

III. Results

Fig. 2 shows the sorted absolute value of the coefficients for each sparsifying transform. We can see that for this data set the wavelet domain is significantly sparser than the commonly used gradient domain.

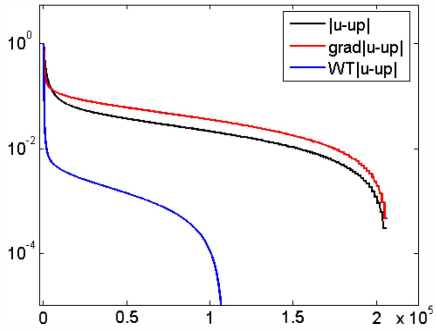

Fig. 2. Sparseness: Sorted absolute values on several transformed domains.

All CS methods eliminated the high noise and severe streak artifacts present in the FDK image due to the lack of projection angles. They also performed very similarly in terms of noise: noise reduction was around 79% measured in an 1800-pixel ROI on the heart area with respect to FDK.

Fig. 3 shows a profile taken across the lung and heart to assess the blurring present in the prior due to the respiratory movement (the white line in the Fig. 3, left). All CS methods showed a good match with the target in respect to resolution, whereas the prior is blurred.

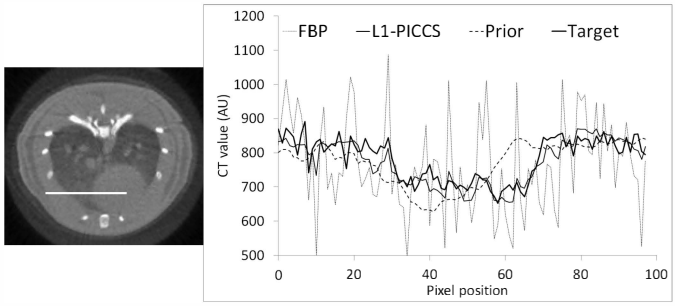

Fig. 3. Left: Central slice of the prior image. Right: Profiles along the white line: low-dose FDK and prior are far from the target, while all CS methods show better fit (only L1-PICCS shown).

Fig. 4 shows the best result for each CS method in terms of mean square error with respect to the high-dose reconstruction (target). TV-PICCS, L1-PICCS and WT-PICCS converged at 40, 25 and 25 iterations respectively.

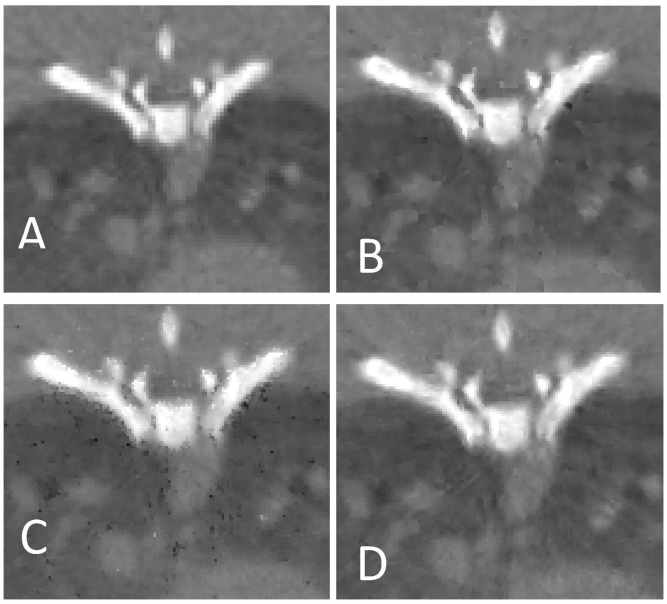

Fig 4. Zoom-in images for target (A), TV-PICCS (B), L1-PICCS (C) and WT-PICCS (D), from left to right and from top to bottom.

From visual inspection, we can appreciate differences in image texture: TV-PICCS (Fig. 4-B) shows a patchy-like pattern and L1-PICCS (Fig. 4-C) shows pixel-like artifact, while WT-PICCS (Fig. 4-D) shows a more natural texture.

IV. Discussion and conclusion

We found that the selection of the sparsity transform for the prior term does not affect resolution and noise performance but it has an influence on the final image texture: Wavelet transform showed a more natural pattern than TV and L1-norm.

There are several limitations and approximations that will be considered in future work. First, in this study we present the results of the three methods for α=0.8 (parameter that weights the prior penalty function), but a study of a wider range of the weighting parameter would be advisable. Second, statistical modeling has been recently shown to improve noise and texture on PICCS [12], and can be easily included within the SB formulation [13]. And finally, we have used a prior based on the union of data for all phase bins, where other priors such as a running average can provide better results [14].

In conclusion, we showed that a compressed sensing methodology using a Split-Bregman approach is feasible to reduce dose in CT with respiratory gating.

References

[1] S. Leng, *et al.*, "High temporal resolution and streak-free four-dimensional cone-beam computed tomography," *Phys Med Biol,* vol. 53, pp. 5653-73, 2008.

[2] S. Sawall, *et al.*, "Low-dose cardio-respiratory phase-correlated cone-beam micro-CT of small animals," *Med Phys,* vol. 38, pp. 1416-24, 2011.

[3] E. J. Candès and J. Romberg, "Practical signal recovery from random projections," *Wavelet Applications in Signal and Image Processing XI, Proc. SPIE Conf,* vol. 5914, 2005.

[4] E. J. Candès, *et al.*, "Robust uncertainty principles: exact signal reconstruction from highly incomplete frequency information," *IEEE Transactions on Information Theory,* vol. 52, pp. 489-509, 2006.

[5] T. Goldstein and S. Osher, "The Split Bregman Method for L1 Regularized Problems," *SIAM Journal on Imaging Sciences,* vol. 2, pp. 323-343, 2009.

[6] J. Tang, *et al.*, "Performance comparison between total variation (TV)-based compressed sensing and statistical iterative reconstruction algorithms," *Phys Med Biol,* vol. 54, pp. 5781-804, 2009.

[7] G. H. Chen, *et al.*, "Prior image constrained compressed sensing (PICCS): A method to accurately reconstruct dynamic CT images from highly undersampled projection data sets," *Medical Physics Letters,* vol. 35, pp. 660-3, 2008.

[8] J. J. Vaquero, *et al.*, "Assessment of a New High-Performance Small-Animal X-ray Tomograph," *IEEE Trans. Nucl. Sci.,* vol. 55, pp. 898-905, 2008.

[9] C. Chavarrías, *et al.*, "Extraction of the respiratory signal from small-animal CT projections for a retrospective gating method," *Phys Med Biol,* vol. 53, pp. 4683-4695, 2008.

[10] J. Abascal, *et al.*, "Fluorescence diffuse optical tomography using the split Bregman method," *Med Phys,* vol. 38, pp. 6275-6284, 2011.

[11] M. Abella, *et al.*, "Software Architecture for Multi-Bed FDK-based Reconstruction in X-ray CT Scanners," *Computer methods and programs in biomedicine,* vol. 107, pp. 218-32, 2012.

[12] P. T. Lauzier, *et al.*, "Time-resolved cardiac interventional cone-beam CT reconstruction from fully truncated projections using the prior image constrained compressed sensing (PICCS) algorithm," *Phys Med Biol,* vol. 57, pp. 2461-76, 2012.

[13] S. Ramani and J. A. Fessler, "A Splitting-Based Iterative Algorithm for Accelerated Statistical X-Ray CT Reconstruction," *IEEE Trans Med Imaging,* vol. 31, pp. 677- 688, 2012.

[14] B. E. Nett, *et al.*, "Perfusion measurements by micro-CT using prior image constrained compressed sensing (PICCS): initial phantom results," *Phys Med Biol,* vol. 55, pp. 2333-50, 2010.